Practical Analysis for Horizontal Diaphragm Design of Wood-Frame Single-Family Dwellings

William J. Kirkham, M.ASCE[1]; Thomas H. Miller, M.ASCE[2]; and Rakesh Gupta, M.ASCE[3]

Abstract: Seismic design of wood-frame single-family dwellings' (WFSFD) lateral force–resisting systems requires determination of the stiffness of horizontal diaphragms and shearwalls. During design, sizes and locations of shearwall openings are often changed, altering shearwall stiffness and loads and requiring a significant redesign effort. Rigid and tributary area method analyses are examined for different geometries of L-shaped WFSFD and include stiffness reductions for roof geometry and pitch. These methods are applied to historic earthquake damage reports and compared using rigid, semirigid, or flexible horizontal diaphragm analyses useful in design practice. Most WFSFD should be designed using an envelope method because they contain a mix of horizontal diaphragm types owing to the effects of roof pitch and geometry on diaphragm stiffness. Cases occur where determination of semirigid or flexible diaphragm behavior is difficult because the analysis results are contradictory or unclear. This suggests that semirigid modeling or an envelope method is prudent. The use of simple rigid plate, flexible plate or semirigid plate methods can be practical for analyzing WFSFD with a reasonable level of detail and effort. **DOI: 10.1061/(ASCE)SC.1943-5576.0000261.**

Author keywords: Diaphragms; Residential buildings; Wood; Wooden structures; Stiffness; Seismic design; Timber construction; Finite-element method; Wood structures; Design.

Introduction

The seismic design of wood-frame single-family dwellings' (WFSFD) lateral force–resisting systems (LFRS) requires determination of the stiffness of diaphragms and shearwalls. In designing WFSFD, it is typical to rearrange or resize openings (windows and doors) changing LFRS's element stiffnesses and changing load distributions. If WFSFD are analyzed with a tributary area method (TAM)/flexible diaphragm method, changes are easily handled; only altered walls need reanalysis. However, TAM ignores torsional effects. Rigid diaphragm methods require extensive reanalysis for each rearrangement because the force distribution for the walls changes. This difference in effort has led some practitioners to advocate flexible diaphragm design as the building code–approved standard in all cases (Qazi 1999). Although WFSFD come in many configurations, design rules of thumb reduce the number of possibilities, so the effects of changes in opening size and location can be more readily evaluated.

Building-code provisions have allowed WFSFD to be designed as flexible diaphragm structures, without the designer determining the relative stiffness of the LFRS elements. Thus, there has been little investigation of how those provisions might affect design if those provisions were required. Investigation of the application of roof pitch and geometry-stiffness reductions from Kirkham et al. (2013) directly affect the determination of LFRS stiffness.

Objectives

The goals of this study were the following:

1. Examine the effects of roof geometry and pitch on LFRS design of WFSFD.
2. Examine existing code provisions for LRFS design in WFSFD to determine areas of concern where strict application of the provisions could be misleading, unconservative, or ambiguous.
3. Compare calculated loads and deflections from TAM, rigid diaphragm analysis by hand, rigid plate finite-element models (RP FEM), and flexible plate finite-element models (FP FEM) to selected WFSFD seismic damage reports.
4. Develop a practical method to evaluate diaphragms of differing stiffnesses with changes in shearwall opening location and size, and to consider torsional effects in WFSFD.

Background

An initial step in the design of LFRS elements of WFSFD is to determine the maximum loads that any LFRS element may experience. For basic structures, *ASCE/SEI 7-10* (ASCE 2010) requires that the structure be analyzed on two perpendicular axes (Section 1.4.3 in ASCE 2010), and typically the larger force shown by analysis for each component becomes the design load for that element. Referring to Fig. 1, using the manual analysis for Wall a, two possible design values, 4.36 kN (980 lbs) and 0.11 kN (25 lbs) are shown. The greater force of 4.36 kN (980 lbs) is the design load.

There are two methods commonly used to determine design loads for WFSFD LFRS elements: TAM and rigid diaphragm analysis (Breyer et al. 2007). Tributary area method assumes that

[1]Principal, APT Engineering, P.O. Box 453, Corvallis, OR 97339 (corresponding author). E-mail: wkirkham@aptengineering.com

[2]Associate Professor, School of Civil and Construction Engineering, Oregon State Univ., Corvallis, OR 97331. E-mail: thomas.miller@oregonstate.edu

[3]Professor, Dept. of Wood Science and Engineering, Oregon State Univ., Corvallis, OR 97331. E-mail: rakesh.gupta@oregonstate.edu

Note. This manuscript was submitted on March 28, 2014; approved on March 13, 2015; published online on June 5, 2015. Discussion period open until November 5, 2015; separate discussions must be submitted for individual papers. This paper is part of the ***Practice Periodical on Structural Design and Construction***, © ASCE, ISSN 1084-0680/04015005(13)/$25.00.

	Rigid Diaphragm Analysis				Flexible Diaphragm Analysis				Maximum
Wall	X-axis accel.	Y-axis accel.	X-axis accel.	Y-axis accel.	X-axis accel.	Y-axis accel.	X-axis accel.	Y-axis accel.	
	RP FEM		Manual		FP FEM		TAM		
	(kN)	(kN)	(kN)	(kN)	(kN)	(kN)	(kN)	(kN)	(kN)
a	**6.38**	0.33	4.36	0.11	4.35	0.02	3.79		6.38
b	1.28	4.12	0.05	**4.52**	0.08	3.52		2.67	4.52
c	0.83	0.10	2.48	0.05	2.76	1.49	**4.37**		4.37
d	0.01	0.09	0.00	0.96	0.22	1.64		**4.37**	4.37
a`	1.53	0.23	**1.98**	0.07	1.64	1.50	0.58		1.98
b`	1.52	**3.72**	0.05	3.55	0.31	2.88		1.71	3.72
Parallel shear	**8.75**	**7.92**	**8.82**	**9.04**	**8.74**	**8.04**	**8.74**	**8.74**	
Perp. shear	**2.81**	**0.66**	**0.10**	**0.23**	**0.61**	**3.00**	**0.00**	**0.00**	
Ratio	**32%**	**8%**	**1%**	**3%**	**7%**	**37%**	**0%**	**0%**	

(1 kN = 225 lbs.)

BOLD are maxima for each wall by any method of analysis

indicates highest two loads for each model type regardless of direction.

Fig. 1. Comparison of diaphragm-analysis methods for Paevere et al. (2003) WFSFD

the diaphragm has zero stiffness. A zero stiffness diaphragm transfers a lateral load to the nearest vertical elements in the LFRS and cannot transfer torsional forces through the diaphragm. A rigid diaphragm analysis locates the center of rigidity (CR) with respect to the LFRS vertical elements and the center of mass (CM) tributary to the diaphragm. The distance between the CR and CM is the diaphragm eccentricity, resulting in torsional forces that increase the seismic demand on some vertical LFRS elements. Where there is concern with the method that is most applicable, some authors recommend performing an *envelope* analysis, using both types of analyses and designing for the greatest force calculated for each element by either method (SEAOC 2006; Breyer et al. 2007). Bearing wall LFRS for WFSFD-containing openings are typically designed by either the perforated shearwall, segmented shearwall, or the force-transfer-around-opening methods (Breyer et al. 2007). Additionally, building codes have traditionally allowed WFSFD to be designed with somewhat less rigorous requirements than other structures (Kirkham 2013).

Building Code Requirements

ASCE/SEI 7-10 (ASCE 2010) allows horizontal wood structural panel diaphragms in WFSFD to be idealized as flexible in Section 12.3.1.1.b (*prescriptive flexible*). In lieu of this, the determination of a flexible diaphragm condition can be made according to Section 12.3.1.3, where a diaphragm is considered flexible if its deflection is at least twice the average drift of adjacent vertical supporting elements under equivalent tributary lateral loading (*calculated flexible*). Section 12.3.1.2 states that certain concrete diaphragms can be idealized as rigid (*prescriptive rigid*). In Section 12.3.1, a diaphragm that meets neither the prescriptive flexible, prescriptive rigid, or calculated flexible-diaphragm conditions must be modeled as *semirigid*. *ASCE/SEI 7-10* (ASCE 2010) provisions that are being investigated (Section 12.3) reference diaphragm flexibility, often as if shearwall flexibility were not being considered. That convention was followed for consistency with the standard.

Finite-Element Models

Though finite-element models (FEM) consider the relative stiffnesses of all LFRS elements, they do not determine a CR or eccentricity of the CR and CM. Thus, it is difficult to apply the torsion required by building codes because there is no direct way to determine how much torsion is already accounted for in the analysis (Goel and Chopra 1993). In nonlinear structural systems, the CR will change location as various resisting elements reach their elastic limits and degrade in stiffness (Kasal et al. 2004). Finite-element models of WFSFD are complex because of irregular shapes and connections between different materials, such as wood to light-gauge steel or wood to concrete. So, no presently available FEM can be used to design complete WFSFD to code requirements with a reasonable level of effort (Skaggs and Martin 2004).

Recent WFSFD Diaphragm Research

The CUREE CalTech Woodframe Project concluded that WFSFD designed with a flexible diaphragm assumption performed better in earthquakes than as rigid diaphragms (Cobeen et al. 2004). This opinion differs from SEAOC (2006) stating that a rigid/flexible diaphragm "…envelope method…will produce more predictable performance than using only flexible or rigid diaphragm assumptions." Schierle (2003) reported seismic damage to five WFSFDs in the 1994 Northridge earthquake, with diagrams showing locations and types of damage; one of the most detailed damage surveys available. Thompson (2000) indicated that most WFSFD would not have flexible diaphragms if the *ASCE/SEI 7-10* (ASCE 2010) criteria were applied.

Ceccotti and Karacabeyli (2002) constructed three-dimensional (3D) FEM with flexible and rigid floor diaphragms using DRAIN 3D. They tentatively concluded that flexible diaphragms have reduced seismic forces and better performance than rigid diaphragms.

Paevere et al. (2003) tested a full-scale WFSFD for lateral wind loads and concluded that the diaphragms behaved rigidly.

Pract. Period. Struct. Des. Constr., 2016, 21(1): 04015005

Kasal et al. (2004) discussed eight different analysis methods by comparing each with a detailed nonlinear FEM calibrated to experiments of Paevere et al. (2003). Among the methods used was a rigid plate model attached to a foundation with springs, based on wind loads applied to the experimental WFSFD. They concluded that TAM was the least accurate in predicting the uplift and shear loads on the experimental WFSFD, and methods including some diaphragm stiffness (i.e., semirigid, semi-flexible) were more accurate.

Kirkham et al. (2013) tested 10 full-scale WFSFD roofs in flat, hip (4:12 pitch), and gable (4:12, 8:12, and 12:12 pitch) configurations. Pitch did not affect roof ultimate strength, but gable roofs were sometimes less than half the stiffness of hip or flat roofs, and the stiffness of gable roofs depended on pitch. Hip roofs showed similar stiffness compared with tested flat roofs and were much stiffer than gable roofs of the same pitch. As many WFSFD are constructed with a gable-roof system, this difference in stiffness can result in significantly different behavior than previously expected.

Geometric Characteristics of WFSFD

Wood-frame single-family dwelling have many shapes and sizes, constructed with different materials and different methods. Lucksiri et al. (2012) characterized the shapes of WFSFD into five categories with the parameters shown in Fig. 2. They examined 412 WFSFD in 10 cities in Oregon, and found that randomly selected L-shaped WFSFDs showed net floor areas varying from 72 to 293 m^2 (780 to 3,150 ft^2); the ratio of the short side to long side, R, varied from 0.48 to 1.0, averaging 0.82, and the ratio of the cutoff area, C_p, varied from 0.03 to 0.31, averaging 0.15.

The CUREE Caltech Woodframe Project documented the condition of a number of buildings after the Northridge earthquake (Schierle 2003). The Smith residence (Fig. 3) is a 115 m^2 (1,240 ft^2) single-story WFSFD. Walls are cement plaster of 1.9 cm (0.75 in.) thick with a 2:12-pitched and 4:12-pitched gable roof. The structure suffered plaster cracking on the front. It is the only example of a true L-shaped, single-story structure in Schierle (2003). It has an R of 0.69 and a C_p of 6%. The Olsen residence (Fig. 4) is a two-story, 261 m^2 (2,810 ft^2) WFSFD, roughly L-shaped with a gable roof having a pitch of 4:12, except 7:12 over the entry. A large portion of the second-level roof slopes toward a first-level living room providing a high ceiling. Walls are cement plaster of 1.9 cm (0.75 in.) thick. Although not strictly L-shaped, the Olsen residence can be idealized as one with an R of about 0.93 and a C_p of about 10% for the first level.

Analysis Methods and Design Implications

In the first portion of this study, analysis was performed on L-shaped WFSFD to examine how the plan geometry and roof pitch affect the application of code provisions and how diaphragm

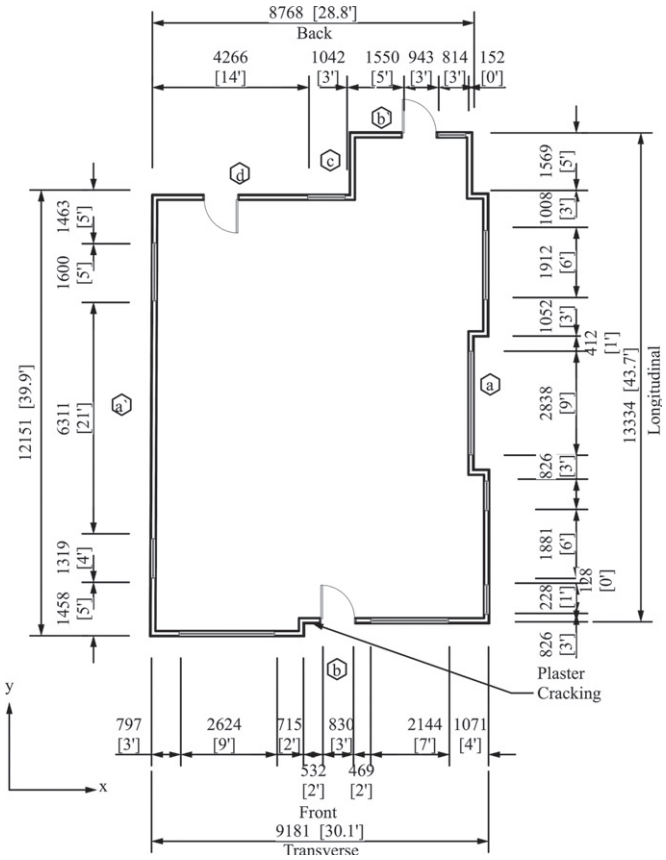

Fig. 3. Smith residence

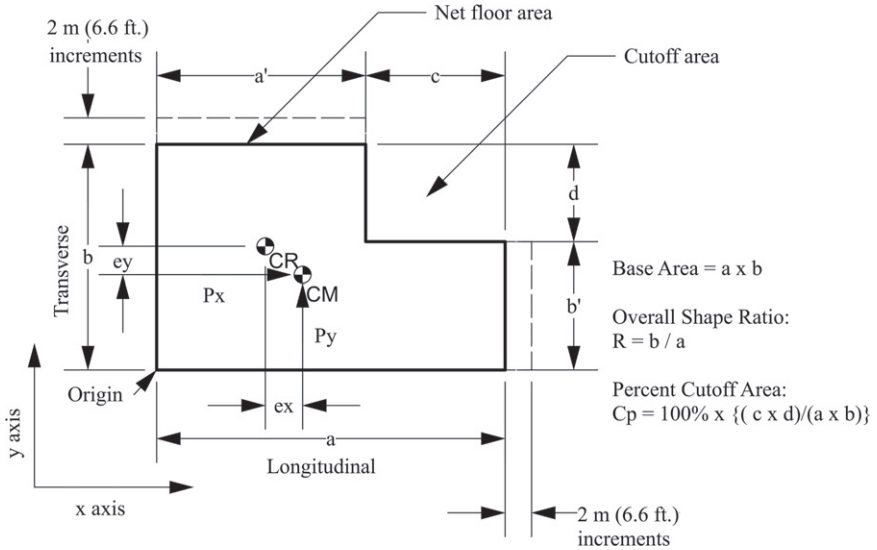

Fig. 2. Shape parameters for L-shaped WFSFD

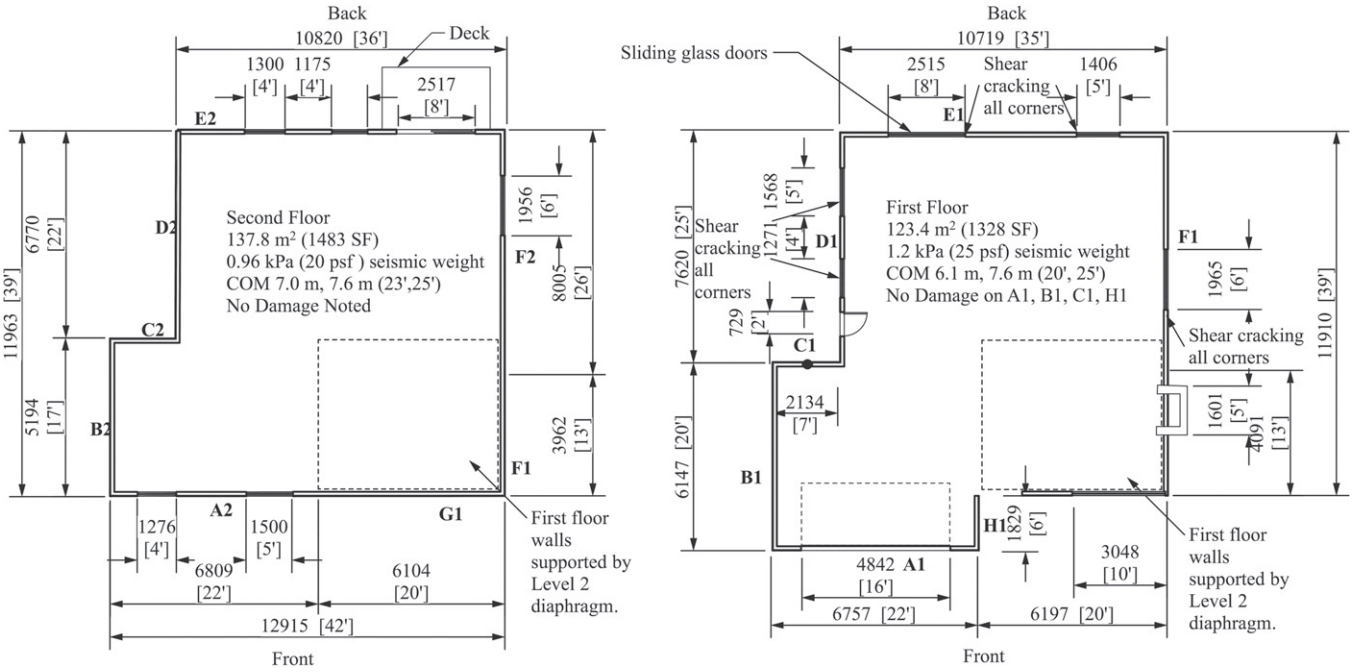

Fig. 4. Olsen residence

flexibility affects LFRS design using conventional methods of WFSFD design. In the second portion of this study, conventional methods of calculating loads in WFSFD were examined and applied to WFSFD damage reported by Schierle (2003), and a practical method considering diaphragm stiffness and torsion in WFSFD was developed. The practical method uses shearwall stiffnesses from perforated shearwall design methods (Sugiyama and Matsumoto 1994) to estimate spring stiffnesses for plate FEM models. The plate stiffnesses were either modeled as flexible, rigid, or semirigid. Semirigid plate (SP) models were calibrated to match the wood-diaphragm deflections calculated from equations in Breyer et al. (2007).

Models were based on the characteristic dimensions and parameters indicated by Lucksiri et al. (2012) (Fig. 2). Walls a and b are the longest, and generally second longest, walls. The longest building axis is the longitudinal axis, and the orthogonal axis is referred to as the transverse axis. Walls a' and b' are the parallel walls opposite the a and b walls, respectively. Walls c and d are referred to as central walls in this paper. An initial model had Wall a equal to 9.75 m (32 ft), Wall b 8.53 m (28 ft), cutout area of Wall c equal to 5 m (16 ft), and Wall d equal to 2 m (6.6 ft). A series of models was then produced increasing Walls b and d in 2-m (6.6 ft) increments to 18.53 m (61 ft) in length, an increase of 220%. Walls a and c remained at the initial conditions. A second set of models began with the initial model and increased lengths of walls a and c in 2-m (6.6 ft) increments to 21.75 m (71.4 ft), an increase of 220%. Walls b and d remained at the initial conditions. These limits were selected because many large urban lots are roughly 30 m (100 ft) on a side, so maximum length of Wall a was only 8.25 m (27 ft) less than the width of a large urban lot. Altogether, 44 models were produced, with three test cases each, for a total of 132 model WFSFDs.

Model Development

Key assumptions included the following:

1. Exterior walls are structural sheathed and full length except for door and window openings.
2. Window area in the exterior walls is 10% of the floor area and evenly distributed to the exterior walls.
3. Exterior doors are at the front and back of the WFSFD. Doors are 1 m (3.3 ft) wide and 2 m (6.6 ft) tall and do not contain windows; therefore, they are not included as a portion of the window area.
4. Wood-frame single-family dwellings are oriented with the major axis parallel to the street or sidewalk; hence, the doors are located on the longest walls of the longest sides (the front door is on Wall a or Wall b and the back door is on Wall a′ or Wall b′).
5. Although windows, doors, and walls have some differences in weight-per-unit area, the difference is neglected in the determination of the CM. Conversely, the stiffness of the walls is reduced by including windows and doors, so the CR is affected by the presence of openings, even if the opening is filled with a window or door.

Diaphragm rigidity depends on a number of geometric factors, so methods have been developed to estimate their stiffness. The Sugiyama and Matsumoto (1994) perforated shearwall method, as shown in Crandell et al. (1999), was used to evaluate the stiffness of the shearwalls. For analyzing many different WFSFD configurations, this method is easiest to implement and is sufficiently accurate. The perforated shearwall design method allows for approximate locations of windows and doors. More exact methods can be used if the locations of openings are precisely known. The Sugiyama and Matsumoto (1994) method uses algebraic formulas to determine strength and stiffness reductions, whereas the Special Design Provisions for Wind and Seismic (SDPWS) code (AF&PA 2009) provides a method to determine the same parameters using tables. Average differences between the algebraic method of Sugiyama and Matsumoto (1994) and the tabular method in SDPWS (AF&PA 2009) varied from 0 to 38% in this study (Kirkham 2013), with an average difference of 12%.

Wood-frame single-family dwelling configurations with three different distributions of window and door openings were used. For Case 1, windows were assumed evenly distributed to each wall on the basis of its portion of the total perimeter, and all windows

were assumed 0.91 m (3 ft) tall. Thus, a wall with 3 m^2 (32 ft^2) of windows would have a length of windows of 3.3 m (11 ft). Wall a had one door and Wall a` (opposite side) had one door; thus, the model has one door on the longest side and one door on the opposite side. Doors are 0.91 m (3 ft) wide by 2 m (6.6 ft) tall. Doors do not have windows, so the door opening area is in addition to the window opening in calculation of the total opening area and length of full-height sheathing. Case 2 was the same as Case 1, except all openings are distributed to Walls a, c, d, and a′. There were no openings on walls b or b as is common for closely spaced WFSFD. Case 3 followed Case 2 assumptions, but additionally assumed the narrower of walls a or b contained the largest garage door, 8.3 or 4.6 m wide (27 or 15 ft), that would fit. Thus, the stiffness of that wall was significantly reduced.

Analysis

The 132 models of WFSFD were generated in a tabular format using Microsoft *Excel*. This permitted detailed implementations of the analysis of each model and ensured the same design methods were used for each. Basic dimensional parameters are the lengths of Shearwalls a, b, c, and d. Characteristic shape parameters R and C_p are calculated from the basic dimensional parameters, as were the net floor area, wall area, and seismic mass. For simplicity, the exterior wall (outside) area is assumed to equal the interior wall (partition) area in the calculation of seismic mass. Seismic design parameters for Portland, Oregon ($S_s = 0.983$, $S_1 = 0.345$) were used, and *ASCE/SEI 7-10* (ASCE 2010) was used to evaluate the seismic load. The service-level seismic load is 8% of the WFSFD mass. The seismic design category was determined to be *D*. Also, as common for light-wood framing, seismic mass includes all walls, regardless of orientation with respect to the direction of seismic acceleration (Breyer et al. 2007). Wall and window areas were determined for each model, and the perforated shearwall adjustment factor was determined for each wall individually, according to Sugiyama and Matsumoto (1994).

Rigid diaphragm analysis and TAM were applied to each analytical model. In the rigid diaphragm analysis, shearwall stiffness was assumed proportional to the length of the wall (Breyer et al. 2007). The rigid diaphragm analysis determined shear loads at the top of the wall due to direct shear and diaphragm torsion and combined those loads for each wall. The loads at the top of each wall were applied to individual walls and to the diaphragms to determine individual shearwall and diaphragm deflections (Breyer et al. 2007). These methods were repeated using TAM for the diaphragms idealized as flexible. Torsional effects determined in the rigid diaphragm analysis were examined to determine their upper and lower bounds. Horizontal irregularities were evaluated using *ASCE/SEI 7-10* Section 12.3 (ASCE 2010). Although some irregularities require use of the redundancy factor, ρ, this usually only affects collectors and has been omitted from this study of forces in shearwalls and diaphragm elements.

The criteria of *ASCE/SEI 7-10* (ASCE 2010) Section 12.3.1.3 were applied to shearwall and diaphragm deflections, and each diaphragm (both orthogonal axes) was determined to be semirigid or flexible.

To evaluate effects of roof diaphragm geometry and pitch, the adjustment factor of Kirkham et al. (2013), identical for each case, was applied to diaphragm deflections, and new determinations of diaphragm flexibility were made for WFSFD cases with a 4:12-pitch gable roof. For gable geometry and 4:12 pitch, roof-diaphragm stiffness was reduced to 40% of the stiffness of a flat roof or a hip roof of the same pitch.

Rigid-plate, FP, and SP FEM model results were compared with the earthquake damage observed by Schierle (2003). The plate model was implemented using *RISA-3D*, which is in common use in small engineering firms with significant features for wood structural design. The plate FEM was a two-dimensional (2D) model of the diaphragm using meshed-plane stress-plate elements with a thickness calibrated to the stiffness of the diaphragm under investigation. The Olsen WFSFD was modeled as two separate 2D plates. Floor plans in Fig. 4 were imported into a computer-aided design program, nodes were exported to a DXF file and then imported into *RISA-3D*. Plate elements were created between nodes, but because *RISA-3D* supports only three-node or four-node isotropic elements/plates, multiple plates were used to assemble each floor model. The RP FEM used a continuous steel plate, 300-mm (11.8 in.) thick to provide rigidity. Linear-elastic wall stiffnesses were determined for individual, generally perforated shearwalls. Shearwalls were modeled as uniaxial springs connected to the diaphragm plate along the wall length with resistance horizontally in the plane of the shearwall. The FP FEM used a steel thickness determined for each model to ensure a calculated flexible condition according to the code definition (ASCE 2010, Section 12.3.1.3). This thickness gave a diaphragm deflection over two times the average wall deflections at that location. Trial and error were required as the distribution of load to the walls depends on diaphragm rigidity relative to the walls. In the RP FEM, nodes along each shearwall were evenly loaded and displaced, owing to the rigidity of the plate. The FP FEM placed no constraints on the nodal relative displacements along each wall, nor did it evenly load those nodes; therefore, tension/compression members (diaphragm chords) were required around the structure's perimeter to provide this constraint. The SP FEM used a thickness selected to provide a diaphragm deflection matching the wood-diaphragm deflection calculated using the equations given in Breyer et al. (2007). This calibration step was the only change required to convert the FP FEM to an SP FEM. There is no real difference in implementation of rigid, flexible, or semirigid diaphragm plate models, except for the inclusion of the required thickness of the plate. Walls schematically outlined in Fig. 5 were not explicitly modeled in the FEM. To perform the simplified analysis on a two-story WFSFD, forces in the uniaxial springs of the second level were summed for each shearwall and applied manually to the wall on the first level. Seismic Loads P1 and P2 were applied to the diaphragm at the center of the diaphragm mass (CM). Springs and plates based on a unit size allowed the resulting loads to be used directly to select shearwall designs from AF&PA

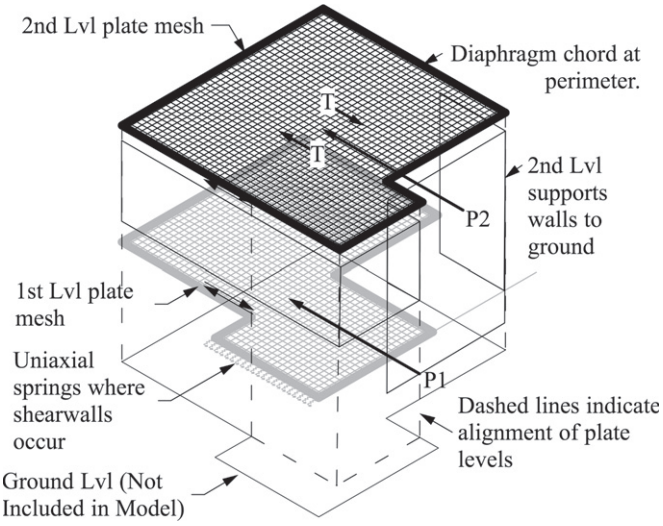

Fig. 5. Plate FEM model for the Olsen residence

(2009) tables. If the designer wishes to add additional torsion to the structure to meet code minimum requirements, it can be added in the form of a couple. Fig. 5 shows a couple on the top level with load arrows marked *T*. The RP, FP, or SP FEM are simple and practical methods that allow engineers to analyze WFSFD with a reasonable level of detail and effort, and are commonly used design/analysis structural-engineering software.

Case Studies of Earthquake Damage

To further investigate the applicability of plate FEM in design, applications were made to cases of documented earthquake damage in WFSFD. Framing is assumed to be nominal 2 × 4 ft (38 × 89 mm) wood studs with doubled studs at the wall ends. Floor-to-floor height is 2.4 m (7.9 ft), with total wood floor thickness of 0.3 m (1 ft). The average wall stiffness is based on tests of stucco walls conducted by the City of Los Angles and the University of California in Irvine (Pardoen et al. 2000). The modulus of elasticity of the diaphragm plates in both models is assumed to be 200,000 MPa (29,000 ksi) and the shear modulus 77,000 MPa (11,200 ksi), typical values for steel rather than wood. Rigid-plate and FP FEM diaphragm stiffnesses are achieved by changing the material thickness. Seismic parameters for Northridge, California, are taken from ZIP Code 91327, near the actual WFSFD locations. Seismic loads are based on diaphragm mass, including the mass of the walls tributary to each diaphragm.

Models include only exterior walls. The effect of stiffness of interior partition walls in a rigid diaphragm analysis is lessened because they are generally closer to the CR unless the structure has significant irregularities. In TAM, including interior walls may result in them being assigned much of the seismic load if the method is rigorously followed. Boundary conditions of designed shearwalls are fairly well understood, but not so for interior partitions. The weaker, interior walls frequently lack hold-downs, rigid support of the wall base, and adequate blocking or bracing to transfer shear from the diaphragm into the interior partition.

Seismic loads are calculated using *ASCE/SEI 7-10* (ASCE 2010), the current code in many areas. Load is applied to each floor level at the diaphragm CM. This is not strictly accurate, but diaphragm mass is generally the larger component in the CM calculations, and wall mass distribution is not usually much different unless substantial openings or different wall construction affects the mass of specific walls.

Results and Discussion

In the following sections, examinations of torsion, diaphragm-flexibility studies, and the structural irregularities noted in the model WFSFD are discussed. Several case studies of the FP, RP, and SP FEM methods are compared with seismic damage reports for those WFSFD.

Observed Torsional Effects

Torsional shear increases for WFSFD from rigid diaphragm analysis were examined. The maximum increase in wall shear was 140% over calculated direct shear for a small Case 3 WFSFD, where the addition of a garage door reduced the stiffness of that wall to near zero (Kirkham 2013). The average increase was 15% for the addition of torsion to direct shear for all three cases.

Diaphragm Flexibility

Determining diaphragm flexibility was more complex than expected. For an L-shaped WFSFD, subdiaphragms were designed as idealized portions of the overall diaphragm (Fig. 6). The L-shaped diaphragm was divided into rectangular subdiaphragms occurring between the shearwalls and collectors. The shearwalls and collectors involved depend on the direction of the lateral force. So, the distribution of seismic loads from Subdiaphragms A, B, C, and D into their supporting shearwalls needed to be evaluated by both rigid analysis and TAM to determine whether each subdiaphragm

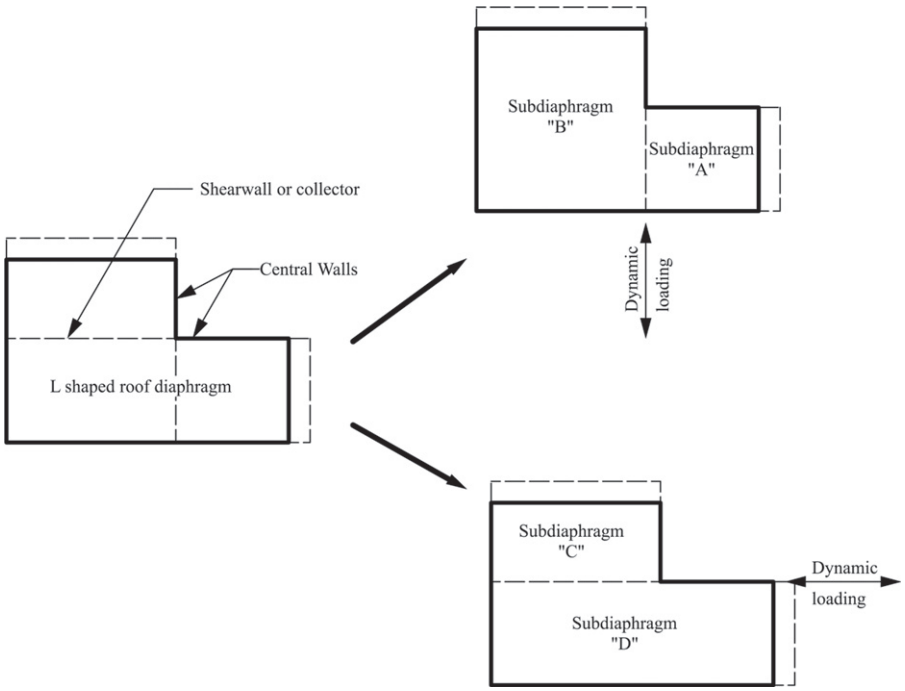

Fig. 6. Modeling an L-shaped diaphragm as four subdiaphragms

Pract. Period. Struct. Des. Constr., 2016, 21(1): 04015005

meets the calculated flexible condition, and then to determine whether the overall diaphragm is calculated as flexible. Even though there are four idealized subdiaphragms shown in Fig. 6, the structure contains only one roof diaphragm. The final roof design was based on the worst case of seismic demand on the four idealized diaphragms.

Model results for individual flat-roof or hip-roof subdiaphragms are shown in Fig. 7(a). For each of the 132 models, there were four subdiaphragms per WFSFD, A, B, C, and D, totaling $132 \times 4 = 528$ individual subdiaphragms. Sixty-two percent of the individual flat-roof subdiaphragms were flexible, whereas 38% were semirigid. Gable roofs with pitches between 4:12 and 12:12 have less stiffness than flat roofs (Kirkham et al. 2013). Using a stiffness reduction of 45% from Kirkham et al. (2013), 4:12 gable-roof subdiaphragms were flexible for 91% of the models, and semirigid for 9%. [Fig. 7(b)]. The change in roof geometry and pitch resulted in a 45% increase in subdiaphragms being calculated as flexible because of the lower stiffness of the 4:12 gable roofs.

This study also examined whether all four of the subdiaphragms for each WFSFD were semirigid or flexible (Fig. 8). For flat or hip roofs [Fig. 8(a)] all four subdiaphragms were flexible for 6% of the models. The 4:12 gable roof results [Fig. 8(b)] showed all four subdiaphragms were flexible in 18% of the models. The greatest percentage of models, 94% of the flat- or hip-roof diaphragms and 82% of the gable roof diaphragms, were a mix of semirigid and flexible subdiaphragms; so both rigid and flexible analyses must be performed to determine loads on the LFRS for design. There were no instances where all four subdiaphragms were semirigid for any pitch. The 18% all flexible in Fig. 8(b) means that four times this many subdiaphragms ($4 \times 18 = 72\%$) were calculated as flexible in Fig. 7(b). The remaining 19% of the diaphragms in Fig. 8(b) ($91 - 72 = 19\%$) were in roof configurations where at least one of the four subdiaphragms was semirigid. The change in roof geometry and pitch to a 4:12 gable roof resulted in a 200% increase [$(18 - 6)/6 = 200\%$] in WFSFD where all four subdiaphragms (A, B, C, and D) were calculated as flexible. The mix of subdiaphragm types and effects of roof pitch and geometry made the analyses more complex. Thus, most WFSFD should be designed using an envelope method, or a method such as the plate

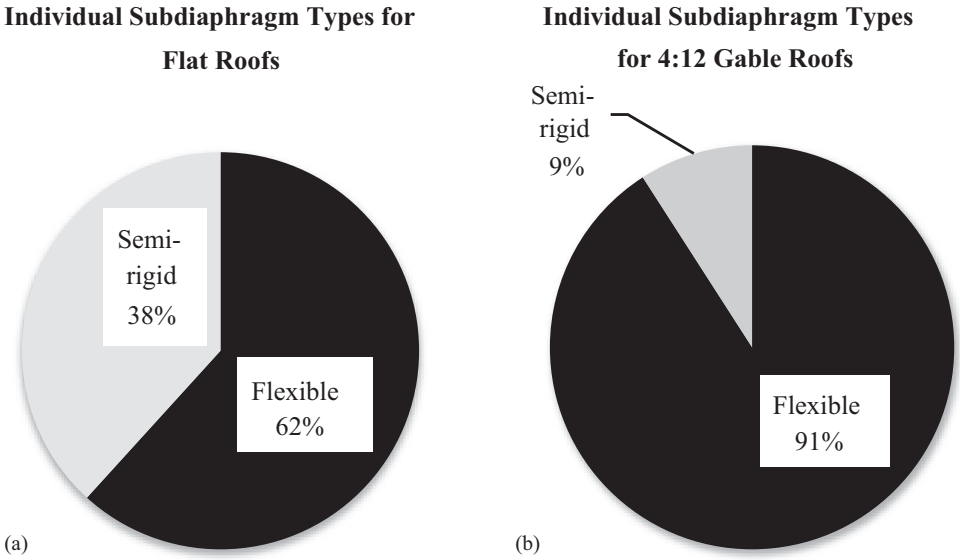

Fig. 7. Evaluation of individual roof subdiaphragms: (a) flat-roof and hip-roof diaphragms; (b) 4:12 gable-roof diaphragms

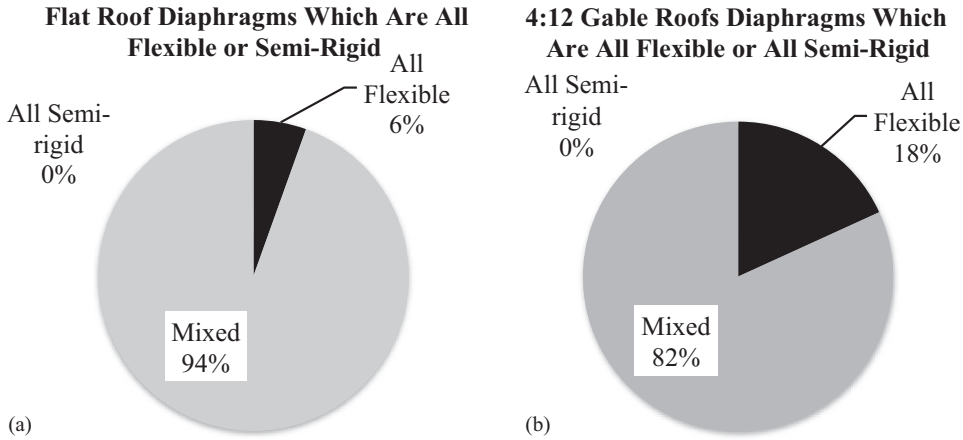

Fig. 8. Portion of WFSFD with all roof subdiaphragms either semirigid or flexible: (a) flat-roof and hip-roof diaphragms; (b) 4:12 gable-roof diaphragms

Pract. Period. Struct. Des. Constr., 2016, 21(1): 04015005

FEM that considers the relative stiffnesses of different LFRS components.

Wood-frame single-family dwelling diaphragms appear to be primarily flexible when the effects of roof pitch and geometry on stiffness are considered, as shown in Fig. 7(b), but an examination of Fig. 8(b) makes it clear that the subdiaphragms are not flexible in all orientations. Designers of WFSFD should consider the effects of roof pitch in determining a calculated flexible diaphragm condition. If the choice of design methods includes only manual rigid-diaphragm analysis or TAM, an envelope analysis is required because the cases that have any rigid subdiaphragms cannot be designed by TAM alone. Further, where increased collector forces are required by code, rigid-diaphragm analysis would be required to determine those forces.

The assumption that WFSFD have flexible diaphragms is valid when some loading directions are considered, but when loads in all orientations are examined, a blanket assumption of flexibility seems unwarranted. If more detailed methods are not used, it is advisable to evaluate WFSFD using an envelope method for both rigid analysis methods and TAM.

To be used in designing, a prescriptive method should have overwhelming support based on the professional judgment of experts or substantially positive supporting research. It should be a method applicable beyond a reasonable doubt. The prescriptive flexible method is supported by Cobeen et al. (2004) and Kasal et al. (2004), but cannot be uniformly assumed accurate according to Thompson (2000), Paevere et al. (2003), Christovasilis and Filiatrault (2010), Phillips et al. (1993), and Skaggs and Martin (2004). Some researchers recommend an envelope method (SEAOC 2006; Breyer et al. 2007). Breyer et al. (2007 have revised a number of paragraphs to consider the new research in this area, and conclude, "Study of the effect of diaphragm modeling choices…is ongoing." Thus, the language of Breyer et al. (2007) is not as supportive of the prescriptive flexible method as Breyer et al. (2003). The prescriptive flexible method no longer has overwhelming expert support or predominantly positive supporting research, and thus there should be further discussion of its appropriate use. Designers should be cautious in using the prescriptive flexible provisions in *ASCE/SEI 7-10* (ASCE 2010), and there should be further discussion of the applicability in light of present opinion.

Diaphragms: Neither Rigid nor Flexible

Some confusing situations arise that should be addressed in future code revisions. To determine whether a diaphragm meets calculated flexible criteria, a WFSFD needs to be evaluated at design loads to determine both diaphragm and shearwall deflections. The distribution of loads from TAM and rigid diaphragm analyses to individual shearwalls can be significantly different. For an instance with central walls where the diaphragm is idealized as flexible, the greatest shear load occurs on the central lateral force–resisting wall when it is aligned with the direction of seismic load application. When the diaphragm is idealized as rigid, the greatest shear loads usually occur on the exterior walls, which are furthest from the CR. Different shearwall loads affect calculated shearwall deflections, thus affecting whether the calculated flexible diaphragm criteria is met. Analyses of diaphragm flexibility using the shear loads distributed by these methods may disagree. Two potential problems can occur:

Diaphragm Is neither Flexible nor Semirigid

Tributary area method may indicate the diaphragm is semirigid, and a rigid diaphragm analysis may indicate that the diaphragm is calculated as flexible. Hence, there is no definitive answer. This occurred in 60% of the 4:12 gable-roof test cases, but obviously this depends on the stiffness of the assemblies involved, so the percentage will vary (Kirkham 2013). To determine if this condition exists, the designer must perform both types of analyses.

Diaphragm Is both Flexible and Semirigid

Tributary area method may indicate a diaphragm is flexible, whereas a rigid diaphragm analysis may indicate that it is semirigid. The designer may be misled to believe that their initial best guess was correct. Designers may not perform the complementary analysis that would reveal the dilemma. Again, to determine if this condition exists, the designer must perform both types of analyses.

Thus, the present methods of analysis by hand do not always lead to definitive results and may leave the designer in a quandary as to how to proceed. Cases may occur where the determination of semirigid or flexible diaphragm behavior is difficult because the code-prescribed analysis is contradictory or unclear. This situation also suggests that the use of SP FEM or a manual envelope method using both rigid diaphragm analysis and TAM is prudent for any WFSFD design.

Structural Irregularities in the Models

Of the model WFSFDs examined, 95% demonstrated Type 1a (Table 12.3-1, ASCE 2010) torsional irregularity and 40% demonstrated Type 1b (Table 12.3-1, ASCE 2010) extreme torsional irregularity (Kirkham 2013). *ASCE/SEI 7-10* (ASCE 2010) prohibits rigid or semirigid diaphragm structures of Type 1b if they are in Seismic Design Category E or F (Section 12.3.3.1, ASCE 2010), and increases collector and connection forces in the LFRS by 25% in Seismic Design Category D (Section 12.3.3.3, ASCE 2010). In Seismic Design Category D, forces are increased, but the structure would be permitted. Three-dimensional representation is required for seismic irregularities of Types 1a, 1b, 4, and 5 (Section 12.7.3, ASCE 2010), including the effects of diaphragm stiffness if semirigid. Torsion needs to be amplified per *ASCE/SEI 7-10* Eqs. (12.8)–(14) (Section 12.8.4.3, ASCE 2010) for most structures, but there is an exception for light-frame structures. Story drift limits for Seismic Design Categories C, D, E, or F are based on the maximum differential drift of vertically aligned points on any edge, including torsional amplification for structures with either Type 1a or 1b irregularities (Section 12.8.6, ASCE 2010).

Re-entrant corner irregularity (Type 2), likely for most L-shaped structures, appeared in 98% of the models (Kirkham 2013). According to ASCE 7 Section 12.3.3.4 (ASCE 2010), LFRS collector and connection design forces need to be increased by 25% for Seismic Design Categories D, E, and F.

Designers should consider the effects of horizontal irregularities in WFSFD. For improved performance of WFSFD, it may be useful to eliminate some of the exceptions included in *ASCE/SEI 7-10* (ASCE 2010) and the IBC (ICC 2012) that permit the design of WFSFD without consideration of torsional effects and re-entrant corner effects.

Analysis by Plate FEM Methods

Seismic damage from the Northridge earthquake is compared with RP FEM, FP FEM, manual rigid diaphragm analyses, and TAM. Rigid diaphragm analysis tends to result in larger shear forces on the exterior and walls furthest from the CR, and those with the greatest stiffness. For an L-shaped WFSFD, it is reasonable to expect that a rigid diaphragm analysis would result in the largest forces on Walls a and b (Fig. 2), which are the longest and most

likely have the greatest stiffness. The next group of walls significantly loaded will be Walls a and b, the next longest walls, probably of intermediate stiffness. Rigid-diaphragm analysis assigns the least load to Walls c and d, which are the shortest walls and also the walls nearest the CR and CM, and which are least affected by torsional forces. Tributary area method assigns most of the load to central Walls c and d.

Paevere et al. House

In Fig. 1, a comparison of results for the Paevere et al. (2003) WFSFD is shown. (See also Fig. 9.) Four analyses were performed: RP FEM, manual rigid-diaphragm analysis, FP FEM, and a flexible diaphragm analysis by TAM. Rigid-plate FEM produced the largest loads to Walls a and b′ (Figs. 2 and 9), the stiffest exterior walls furthest from the CR. The greatest loads by any method were from the rigid-diaphragm analyses. Tributary area method showed the highest loads on Walls c and d, as expected. In any flexible diaphragm with two spans, half of the diaphragm load on each span is applied at the central wall. Thus, central Wall c receives a load equal to the sum of the shear loads on Walls a and a′, and similarly, Wall d receives loads from Walls b and b′.

Tributary area method will often over predict loads on central walls if diaphragms are treated as simple spans between parallel shearwalls, and as a result, loads on the exterior walls may be too low (Fig. 1). Damage surveys (Schierle 2003) showed significant damage on the exterior walls of the subject WFSFD, more consistent with results of the rigid-diaphragm methods. Both plate FEM methods and the manual rigid-diaphragm analysis distributed the highest two loads per method to the longest/stiffest, exterior walls a and b. Flexible plate FEM distributed more load than RP FEM to the central walls, reflecting flexible diaphragm behavior.

In Fig. 1, both FEM and rigid diaphragm manual analysis showed effects of torsional loading. For x-axis acceleration RP FEM, FP FEM, and manual rigid diaphragm analyses, walls a, c, and a′ were parallel to the direction of loading, so most of their loading was direct shear. The loads shown on walls b, d, and b′, that were perpendicular to the x-axis acceleration, showed loads that were solely due to torsional effects. The ratio of parallel to perpendicular shear gives an indication of the torsional effect. Only the commonly used TAM did not show any torsion. Although not directly calculated using TAM, the FP FEM allows inclusion of an additional torsional load if needed by applying a couple as shown in Fig. 5.

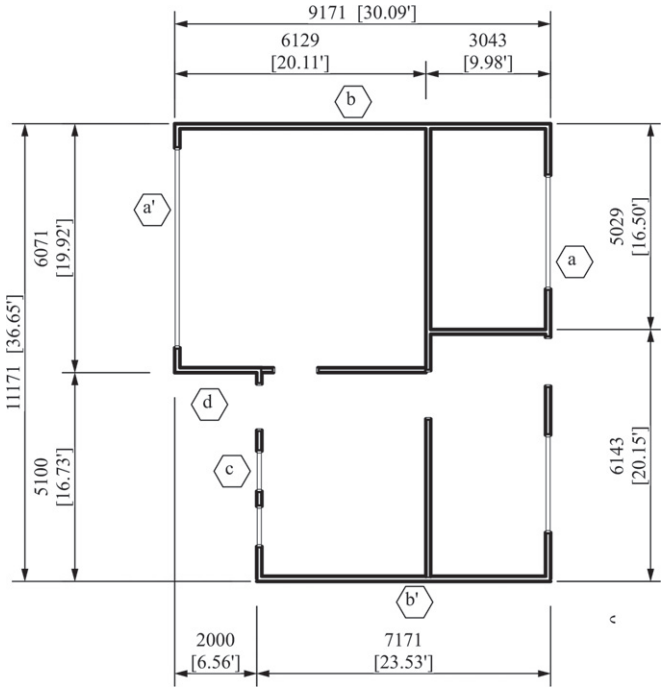

Fig. 9. Paevere et al. (2003) house

Smith Residence

The Smith residence (Fig. 3) was evaluated using both the RP and FP FEM. Plate thickness for the FP FEM model was determined by trial analyses until the diaphragm for both orthogonal axes met the calculated flexible criterion. Though the code criterion indicates the RP FEM model is semirigid, as discussed under the section "Building code requirements," the model was intended to be so stiff as to be comparable to the manual rigid-analysis method. *ASCE/SEI 7-10* (ASCE 2010) provides prescriptive flexible and rigid conditions, and calculated flexible conditions, and there is no calculated rigid condition. Therefore, only engineering judgement can be used to determine whether a semirigid model can be approximated by a manual rigid-diaphragm analysis. Both RP and FP FEM for the Smith residence showed wall end deflections on the transverse axis (Walls b, b′, and d over twice those of the longitudinal axis (Walls a, a′, and c) (Fig. 3). Further, the greatest diaphragm deflection occurred at midspan of the diaphragm for y-axis seismic loading in both models, but the only damage on the actual structure (Schierle 2003) was on the front, which the authors suspect was caused by x-axis loading. Thus, the midspan and wall deflections of the models did not appear consistent with the reported seismic damage on the Smith residence. It is possible that the cracking reported was not due to in-plane shearwall deflection, but may be due to some other mechanism of damage. But at present, the methods examined in this study for estimating building component loads and deflections do not appear to correlate with observed damage.

In Fig. 10, wall loads from applying the five calculation models to the Smith residence are shown. The largest load values were on Walls b and a′ in the manual rigid diaphragm, RP FEM, SP FEM, and FP FEM, and on Walls c and d using TAM. Although the diaphragm may be prescriptively flexible according to *ASCE/SEI 7-10* [Section 12.3.11(b), ASCE 2010], the FP FEM diaphragm still has some stiffness and therefore develops some torsion and redistributes a portion of the seismic load to elements depending on rigidity. The manual rigid-diaphragm analysis provided the lowest design loads on the central Walls c [0.79 kN (180 lbs)] and d [4.66 kN (1.05 kip)], and high design loads on exterior Walls a [6.25 kN (1.41 kip)], b [11.9 kN (2.66 kip)], a′ [10.2 kN (2.29 kip)] and b′ 8.25 kN (1.86 lbs)]. Design practice involves determining shearwall unit loads and then designing each shearwall for the required unit load (Breyer et al. 2007). The rightmost column of Fig. 10 shows the envelope analysis [maximum unit load from among manual rigid diaphragm, RP, SP FEM, FP FEM, and TAM]. Damage reported by Schierle (2003) on this WFSFD was on Wall b. The RP, SP, FP FEM, and manual rigid diaphragm methods all provided high design loads for Wall b, the most damaged wall, but the envelope analysis shows that the unit shear on Wall b was not the most highly loaded wall. The highest load on Wall b by these four methods was from the manual rigid diaphragm method, but it was at most 20% higher than the largest load from each of the other four methods, so all four methods were comparable. The fifth method, TAM, also indicated a high load on Wall b but showed the highest loads on central Walls c and d, which were undamaged. Wall b was not ranked as a wall with a high unit load by any of the analysis methods used in this study; thus, their effectiveness in predicting damage was not demonstrated in this case.

Wall	Rigid Diaphragm Analysis				Flexible Diaphragm Analysis				Semi-Rigid		Max. Total Load	Max. Unit Load
	X-axis accel.	Y-axis accel.	X-axis accel.	Y-axis accel.	X-axis accel.	Y-axis accel.	X-axis accel.	Y-axis accel.	X-axis accel.	Y-axis accel.		
	RP FEM		Manual		FP FEM		TAM		SP FEM			
	(kN)	(kN)	(kN)	(kN)	(kN)	(kN)	(kN)	(kN)	(kN)	(kN)	(kN)	(kN/m)
a	7.98	0.97	6.25	5.14	**9.73**	0.00	4.50	0.00	9.54	0.39	9.73	0.73
b	1.07	9.92	1.01	**11.85**	2.41	10.99	0.00	10.14	1.88	10.32	**11.85**	1.29
c	2.25	0.14	0.79	0.28	3.01	0.30	**10.68**	0.00	2.94	0.25	10.68	1.92
d	0.62	7.71	1.58	4.66	0.86	8.72	0.00	**10.68**	0.86	8.33	10.68	1.64
a`	**11.21**	1.25	10.17	0.60	9.79	0.00	6.17	0.00	9.79	0.53	11.21	0.92
b`	0.40	3.65	1.21	**8.25**	0.60	2.05	0.00	0.53	0.50	2.70	8.25	**2.39**
Parallel shear	21.44	21.28	17.21	24.76	22.53	21.76	21.35	21.35	22.26	21.35		
Perp. shear	2.10	2.36	3.79	6.02	3.87	0.30	0.00	0.00	3.23	1.18		
Ratio	10%	11%	22%	24%	17%	1%	0%	0%	15%	6%		

(1 kN = 225 lbs., 1 kN/m = 68.5 lbs./ft.)

BOLD are maxima for each wall by any method of analysis

indicates highest two loads for each model type regardless of direction.

Fig. 10. Comparison of diaphragm analysis methods for Smith residence; plans and descriptions of damage from Schierle (2003)

These results demonstrate that an envelope method using rigid and flexible diaphragm–analysis methods did encompass all maximum loads. By comparing the SP FEM model with the maximum loads shown on Walls a, b, a' and b′ in Fig. 10, it can be demonstrated that an SP FEM will produce lower design loads than the envelope method if knowledge of diaphragm stiffness is adequately reflected in the model. The envelope method is a reasonable approach where true diaphragm behavior is not understood, but may result in overdesign of some elements. The SP FEM total direct-shear design loads are equal to or greater than those of TAM.

Olsen Residence

Application of RP and FP FEM to the Olsen residence (Fig. 4) is shown in Figs. 11 and 12. Wall deflections are shown in Fig. 11 for each wall and building level. Bold and shaded numbers show deflections exceeding 24 mm (0.95 in.), the recommended 1% story maximum drift to reduce the risk of damage (Pardoen et al. 2000). Neither method suggested any damage to the walls on Level 2 based on deflection, consistent with the damage report (Schierle 2003). On Level 1, FP FEM deflections suggest damage to five walls, but two of the walls (B1, C1) have no reported damage, and on one wall (E1) that had damage, the FP FEM assigns the lowest drift (but just 10% below the damage criterion). So, the applicability of FP FEM to correctly describe the damage potential is unclear. The RP FEM predicts no damage to Level 1 walls; however, the wall with the highest drift (A1) was behind brick veneer and the damage could have been concealed from view.

Schierle (2003) indicated no damage to any Level 2 wall, but recorded damage to Level 1 Walls D1, E1, and F1. It is possible that there was concealed damage behind the brick veneer, or that the veneer provided sufficient additional stiffness (not in the models) to prevent damage on Walls A1 and G1. Without quantitative differentiation of deflection around the structure, it is difficult to verify the computational models as predictors of damage.

In Fig. 12, calculated loads are presented from the RP and FP FEM models. Seismic loads are applied on each orthogonal axis, and the maximum load for each wall is then summarized as the design load for that wall. There is no damage reported for Level 2 (Schierle 2003), so the table is limited to Level 1. The average wall load for x-axis loading of the FP FEM is 76.0 kN (17.1 kip)/7 walls or 10.9 kN (2.45 kip) per wall. All three damaged walls, D1, E1, and F1, have calculated design loads above the average wall load for the FP FEM, and 61% of the total design load was applied to walls with reported damage. Design is performed using the greater of the unit loads calculated on each axis (Breyer et al. 2007). The FP FEM model indicates the two highest unit loads on Walls C1 and H1, which have no recorded damage.

For the RP FEM analysis, two of the three most highly loaded walls, E1 and F1, had reported damage, and 54% of the total Level 1 RP design load [76.0 kN (17.1 kip)] was applied to these two damaged walls. The highest wall loads for the FP FEM were on all three of the damaged walls, and these walls carried 61% of the total design load of 76.0 kN (17.1 kip). The highest design unit load occurred on damaged Wall E1, with the remaining damaged walls at loads below the average. Thus, in this case, the RP FEM provided higher unit-shear loads on at least one damaged wall and so better predicted the observed damage, in a limited sense.

Pract. Period. Struct. Des. Constr., 2016, 21(1): 04015005

			Wall	Deflection		
				X-Axis Seismic (mm)	Y-Axis Seismic (mm)	Max. (mm)
LEVEL 2	FP FEM	X-Axis Seismic	A2	7	10	10
			B2	11	3	11
			C2	11	5	11
			D2	9	6	9
			E2	8	21	21
			F2	23	6	23
			F1	14	6	14
			G1 §	7	16	16
	RP FEM	X-Axis Seismic	A2	8	5	8
			B2	8	5	8
			C2	8	5	8
			D2	8	5	8
			E2	8	6	8
			F2	8	6	8
			F1	8	6	8
			G1 §	8	6	8
LEVEL 1 *	FP FEM	X-Axis Seismic	A1 §	24	12	24
			B1	35	4	**35**
			C1	43	10	**43**
			D1	42	17	**42**
			E1	13	23	23
			F1	39	8	**39**
			H1	28	13	**28**
	RP FEM	X-Axis Seismic	A1 §	23	9	23
			B1	21	8	21
			C1	19	8	19
			D1	17	8	17
			E1	15	9	15
			F1	18	10	18
			H1	22	9	22

(25.4 mm = 1 inch)
BOLD wall identifiers indicate walls with observed damage.
BOLD SHADED walls with drift > 1% at wall top.
* Level 2 loads were from the FP FEM load case above.
§ Indicates wall with partial or full brick veneer.

Fig. 11. Olsen residence wall deflections; plans and descriptions of damage from Schierle (2003)

If an envelope analysis using the greater load for each wall from either the RP or FP FEM, is used, the total design load is 88.6 kN (20.0 kip), with an average wall load of 12.7 kN (2.86 kip). Again, only Walls E1 and F1 (two of the three damaged walls) are above the average. However, the three greatest loads are on Walls D1, E1, and F1, the three damaged walls. Design-unit loads for the envelope analysis are highest on Walls C1, H1, and E1, only one of which had observed damage. Thus, both the RP FEM and envelope FEM methods have one their three highest loads on a damaged wall, whereas the FP FEM has none. When it is unclear whether the diaphragms are flexible, an envelope analysis is prudent because of the limited accuracy of damage predictions from any of the methods.

None of the methods examined consistently predicted high displacements or high unit-shear loads on walls with the greatest damage in the 1994 Northridge earthquake residences. In Figs. 1 and 10, TAM is the only method that distributes the largest design loads to the central walls. Plate FEM and manual rigid-diaphragm analysis effectively considers the relative stiffnesses of diaphragms and shearwalls.

Conclusions and Recommendations for Design

Envelope Method

Cases may occur where determination of semirigid or flexible diaphragm behavior is difficult as the code-prescribed analysis is contradictory or unclear. This suggests that use of SP FEM or a manual envelope method using both rigid diaphragm analysis and the TAM is prudent for WFSFD design. The mix of subdiaphragm types and effects of roof pitch and geometry make the analyses more complex. Tributary area method often over predicts loads on central walls if diaphragms are treated as simple spans between parallel shearwalls, and as a result, loads on the exterior walls may be too low.

Flexible Diaphragm Assumption

The assumption that WFSFD have flexible diaphragms has basis when some loading directions are considered, but when loads in all orientations are examined, a blanket assumption of flexibility seems unwarranted. The prescriptive flexible method no longer has overwhelming expert support or predominantly positive supporting research, and there should be further discussion of its appropriate use. Designers should also consider effects of horizontal irregularities in WFSFD. It may be useful to eliminate exceptions included in *ASCE/SEI 7-10* (ASCE 2010) and the IBC (ICC 2012) that permit WFSFD design without considering torsional effects and re-entrant corner effects.

Practical Method Using Plate FEM

Flexible-plate FEM makes it possible to apply a torsional load, although this loading is not easily included in TAM. A SP FEM will produce lower design loads than the envelope method if knowledge of diaphragm stiffness is adequately reflected in the model.

The RP, FP, or SP FEM methods are simple and practical methods for an engineer's toolbox to analyze WFSFD with a reasonable level of detail and effort, and commonly used design/analysis structural engineering software. There is no real difference in implementation of rigid, flexible or semirigid diaphragm plate models, except for inclusion of the required thickness of the plate. Plate FEM methods and manual rigid diaphragm analysis are the only methods that consider the stiffnesses of the shearwalls. Combining the perforated shearwall stiffness method with a calibrated plate FEM allows evaluation of diaphragms with different stiffnesses, permits changes of shearwall openings and sizes and consideration of torsional effects in the structure.

None of the methods examined consistently predicted high displacements or high unit loads on walls with the greatest damage in 1994 Northridge earthquake residences, and thus their effectiveness in predicting and modeling damage has not been demonstrated.

Recommendations

Designers of WFSFD should consider the effects of roof pitch in determining a calculated flexible–diaphragm condition. They should also be wary of using the prescriptive flexible provisions in *ASCE/SEI 7-10* (ASCE 2010), and there should be further discussion of the applicability in light of present opinion. Wood-frame single-family dwelling should be designed using an envelope method, or a method such as the plate FEM that considers the stiffnesses of different LFRS components. In determining whether a calculated flexible condition exists, both

			Wall	Length (m)	Unit Load (kN/m)	Load (kN)
LEVEL 1 *	FP FEM	X-Axis	A1	6.71	1.58	10.57
			B1	5.18	0.55	-2.87
			C1	2.13	3.66	7.82
			D1	6.78	0.66	4.45
			E1	11.13	2.03	22.57
			F1	7.92	0.61	4.86
			H1	1.83	1.33	2.43
			Total			41.80
		Y-Axis	A1	6.71	0.15	0.98
			B1	5.18	0.99	5.14
			C1	2.13	0.34	0.72
			D1	6.78	1.78	12.07
			E1	11.13	0.01	0.16
			F1	7.92	1.49	11.80
			H1	1.83	3.30	-6.03
			Total			35.15
	RP FEM	X-Axis	A1	6.71	1.50	10.08
			B1	5.18	0.72	3.71
			C1	2.13	1.63	3.49
			D1	6.78	0.18	1.19
			E1	11.13	2.45	27.28
			F1	7.92	0.67	5.32
			H1	1.83	0.16	0.29
			Total §			41.56
		Y-Axis	A1	6.71	0.10	0.69
			B1	5.18	2.12	10.96
			C1	2.13	0.06	0.12
			D1	6.78	0.90	6.14
			E1	11.13	0.06	0.65
			F1	7.92	1.75	13.88
			H1	1.83	2.29	4.19
			Total §			35.33

Wall	Design Unit Load (kN/m)	Design Load (kN)
A1	1.58	10.57
B1	0.99	5.14
C1	**3.66**	7.82
D1	1.78	**12.07**
E1	2.03	**22.57**
F1	1.49	**11.80**
H1	**3.30**	6.03
Total		76.00

Wall	Design Unit Load (kN/m)	Design Load (kN)
A1	1.50	10.08
B1	**2.12**	**10.96**
C1	1.63	3.49
D1	0.90	6.14
E1	**2.45**	**27.28**
F1	1.75	**13.88**
H1	**2.29**	4.19
Total		76.01

Wall	Envelope Unit Loads (kN/m)	Envelope Design Loads (kN)
A1	1.58	10.57
B1	2.12	10.96
C1	**3.66**	7.82
D1	1.78	12.07
E1	**2.45**	**27.28**
F1	1.75	**13.88**
H1	**3.30**	6.03
Total		88.61

(1 kN = 225 lbs., 1 kN/m = 68.52 lbs./ft.)
BOLD wall identifiers indicate walls with observed damage.
BOLD and shaded numbers are walls with loads above the average of all walls.

* Level 2 loads transferred to Level 1 were the "Flexible" load case above.

§ Total base shear is 43.2 kN (9.70 kips), but walls F2 and G1 are not included in this total, hence the discrepancy. See Fig. 5.

Fig. 12. Calculated loads for Olsen residence by FP and RP; plans and descriptions of damage from Schierle (2003)

rigid and TAM must be used. When it is not clear whether WFSFD diaphragms are flexible, an envelope analysis is prudent.

References

AF&PA (American Forest and Paper Association). (2009). *Special design provisions for wind and seismic with commentary—2008*, Washington, DC.

ASCE. (2010). "Minimum design loads for buildings and other structures." *ASCE/SEI 7-10*, Reston, VA.

Breyer, D. E., Fridley, K. J., Cobeen, K. E., and Pollock, D. G. (2007). *Design of wood structures ASD/LRFD*, 6th Ed., McGraw-Hill, New York.

Breyer, D. E., Fridley, K. J., Pollock, D. G., and Cobeen, K. E. (2003). *Design of wood structures ASD*, 5th Ed., McGraw-Hill, New York.

Ceccotti, A., and Karacabeyli, E. (2002). "Validation of seismic design parameters for wood-frame shearwall systems." *Can. J. Civil Eng.*, 29, 484–498.

Christovasilis, I. P., and Filiatrault, A. (2010). "A two-dimensional numerical model for the seismic collapse assessment of light-frame wood structures." *Structures Congress 2010*, S. Senapathi and K. Casey, eds., ASCE, Reston, VA, 832–843.

Cobeen, K., Russell, J., and Dolan, J. D. (2004). "Recommendations for earthquake resistance in the design and construction of woodframe buildings, Part I: Recommendations." *Rep. No. W-30a*, CUREE, Richmond, CA.

Crandell, J., Freeborne, W., and McKee, S. (1999). "Perforated shear walls with conventional and innovative base restraint connections." *Proc., Joint Meeting US–Japan Cooperative Program in Natural Resources Panel on Wind and Seismic Effects*, M. Okahara, ed., Vol. 31, Public Works Research Institute, Tsukuba-shi, Ibaraki-ken, Japan, 433–429.

Goel, R. K., and Chopra, A. K. (1993). "Seismic code analysis of buildings without locating centers of rigidity." *J. Struct. Eng.*, 10.1061/(ASCE)0733-9445(1993)119:10(3039), 3039–3055.

ICC (International Code Council). (2012). *2012 International building code*, Country Club Hills, IL.

Kasal, B., Collins, M. S., Paevere, P., and Foliente, G. C. (2004). "Design models of light frame wood buildings under lateral loads." *J. Struct. Eng.*, 10.1061/(ASCE)0733-9445(2004)130:8(1263), 1263–1271.

Kirkham, W. J. (2013). *Examination of lateral stiffness and strength of pitched residential roof diaphragms with implications for seismic design*, Oregon State Univ., Corvallis, OR.

Kirkham, W. J., Gupta, R., and Miller, T. H. (2013). "Effects of roof pitch and gypsum ceilings on the behavior of wood roof diaphragms." *J. Perform. Constr. Facil.*, 10.1061/(ASCE)CF.1943-5509.0000490, 04014039.

Lucksiri, K., Miller, T. H., Gupta, R., Pei, S., and van de Lindt, J. W. (2012). "Effect of plan configuration on seismic performance of single-story wood-frame dwellings." *Nat. Hazard. Rev.*, 10.1061/(ASCE)NH.1527-6996.0000061, 24–33.

Paevere, P. J., Foliente, G. C., and Kasal, B. (2003). "Load-sharing and redistribution in a one-story woodframe building." *J. Struct. Eng.*, 10.1061/(ASCE)0733-9445(2003)129:9(1275), 1275–1284.

Pardoen, G., et al. (2000). "Results from the city of Los Angeles–UC Irvine shear wall test program." *6th World Conf. on Timber Engineering*, Venue West Conference Services, Vancouver, BC.

Phillips, T. L., Itani, R. Y., and McLean, D. I. (1993). "Lateral load sharing by diaphragms in wood-framed buildings." *J. Struct. Eng.*, 10.1061/(ASCE)0733-9445(1993)119:5(1556), 1556–1571.

Qazi, S. (1999). *SEAINT Wood Design–Wood Panel Rep.*, ⟨http://www.seaint.org/wood.htm⟩ (Feb. 24, 2014).

RISA-3D Version 13 [Computer software]. Foothill Ranch, CA, RISA Technologies.

Schierle, G. G. (2003). "Northridge earthquake field investigations: Statistical analysis of woodframe damage." *Rep. No. W-09*, CUREE, Richmond, CA.

SEAOC (Structural Engineers Association of California). (2006). *2006 IBC structural/seismic design manual*, Sacramento, CA.

Skaggs, T. D., and Martin, Z. A. (2004). "Estimating wood structural panel diaphragm and shear wall deflection." *Pract. Period. Struct. Des. Constr.*, 10.1061/(ASCE)1084-0680(2004)9:3(136), 136–141.

Sugiyama, H., and Matsumoto, T. (1994). "Empirical equations for the estimation of racking strength of plywood-sheathed shear walls with openings." *Summaries of Technical Papers of Annual Meeting*, Transactions of the Architectural Institute of Japan, Tokyo, Japan.

Thompson, D. S. (2000). "Wood diaphragm and shear wall deflections." *Structures Congress 2000: Advanced Technology in Structural Engineering*, M. Elgaaly, ed., ASCE, Reston, VA, 1–9.